PiB-Conjugated, Metal-Based Imaging Probes: Multimodal Approaches for the Visualization of β-Amyloid Plaques

André F. Martins,[†,‡] Jean-François Morfin,[†] Anna Kubíčková,[†,§] Vojtěch Kubíček,[†] Frédéric Buron,[‖] Franck Suzenet,[‖] Milena Salerno,[⊥] Adina N. Lazar,[#] Charles Duyckaerts,[#] Nicolas Arlicot,[¶] Denis Guilloteau,[¶] Carlos F. G. C. Geraldes,*[,‡] and Éva Tóth*[,†]

[†]Centre de Biophysique Moléculaire, CNRS, Rue Charles Sadron, 45071 Orléans Cedex 2, France

[‡]Department of Life Sciences, Center of Neurosciences and Cell Biology (CNC), and Coimbra Chemistry Center, University of Coimbra, Portugal

[§]Department of Analytical Chemistry, Charles University in Prague, Albertov 2030, 12840 Prague, Czech Republic

[‖]Institut de Chimie Organique et Analytique, UMR 7311 CNRS/Université d'Orléans, rue de Chartres, 45067 Orléans, France

[⊥]Laboratoire CSPBAT, CNRS UMR 7244, UFR-SMBH, Université Paris 13, 74 rue Marcel Cachin, 93017 Bobigny, France

[#]Centre de Recherche de l'Institut du Cerveau et de la Moelle, CNRS UMR7225, INSERM, UMR975 and UPMC, Hôpital de la Pitié-Salpêtrière 47, Bd de l'Hôpital 75013 Paris, France

[¶]Inserm, U930, Université François Rabelais de Tours, CHRU de Tours, 37044 Tours Cedex 9, France

S *Supporting Information*

Gd^{3+}: MRI
^{111}In^{3+}: SPECT

PiB — 6F3D — merge

Eu(DO3A-PiB) — 6F3D — merge
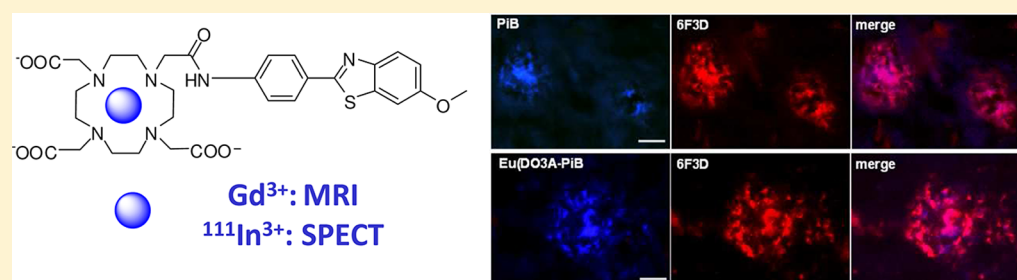
ABSTRACT: In an effort toward the visualization of β-amyloid plaques by in vivo imaging techniques, we have conjugated an optimized derivative of the Pittsburgh compound B (PiB), a well-established marker of Aβ plaques, to DO3A-monoamide that is capable of forming stable, noncharged complexes with different trivalent metal ions including Gd^{3+} for MRI and ^{111}In^{3+} for SPECT applications. Proton relaxivity measurements evidenced binding of Gd(DO3A-PiB) to the amyloid peptide Aβ$_{1-40}$ and to human serum albumin, resulting in a two- and four-fold relaxivity increase, respectively. Ex vivo immunohistochemical studies showed that the DO3A-PiB complexes selectively target Aβ plaques on Alzheimer's disease human brain tissue. Ex vivo biodistribution data obtained for the ^{111}In-analogue pointed to a moderate blood−brain barrier (BBB) penetration in adult male Swiss mice (without amyloid deposits) with 0.36% ID/g in the cortex at 2 min postinjection.

KEYWORDS: imaging agents, Gd^{3+}, ^{111}In^{3+}, amyloid plaques, Alzheimer's disease, Pittsburgh compound B

Alzheimer's disease (AD) is a chronic neurodegenerative disorder leading to progressive decline of cognitive functions.[1−3] Characteristic neuropathological findings associated with AD include the formation of extracellular senile plaques containing β-amyloid peptides and neurofibrillary tangles.[4−6] Currently, no clinical imaging techniques are available for early detection of AD. Thus, the development of diagnostic agents for early in vivo visualization of the amyloid plaques is a critical issue, which would also be important for monitoring new therapies. Significant advances have been made in the field of nuclear imaging, in particular in positron emission tomography (PET). Small organic compounds such as derivatives of thioflavin T, benzoxazoles, and stilbenes have high binding affinities for the Aβ aggregates and some of them

pass the blood−brain barrier (BBB). They inspired the development of amyloid-labeling nuclear imaging probes.[7−11] [11]C- and ^{18}F-labeled derivatives of stilbene[9] and the Pittsburgh compound-B (PiB)[7,8] are promising PET tracers of AD; certain compounds are making their way into the clinics.[8−10] Attempts have been also made to develop ^{99m}Tc-labeled Aβ SPECT probes, which, given the easier accessibility of ^{99m}Tc as compared to ^{18}F, could provide a more convenient approach to the detection of AD. Small, neutral ^{99m}Tc-probes have been reported based on derivatives of biphenyl,[12] benzothiazole

aniline,[13] chalcone,[14] flavone,[15] or pyridyl benzofurane.[16] Some showed reasonable brain uptake and affinity toward β-amyloid plaques.[16]

Magnetic resonance imaging offers noninvasive mapping of structure and function with excellent spatial resolution. MR contrast can be enhanced with paramagnetic contrast agents (CAs), ideally with specific and selective delivery. Gd^{3+} complexes are the most widely used contrast materials.[17] In the absence of any CA, the MR contrast in the amyloid plaques is associated to iron accumulation, which leads to hypointense spots in T_2, T_2^* or susceptibility-weighted images.[18] The detection of plaques weakly loaded with iron is more challenging, and exogenous contrast agents become necessary. So far, the development of MRI contrast agents for the diagnosis of Alzheimer's disease has been modest. Poduslo et al. visualized AD plaques with GdDTPA conjugated to a putrescine-modified human $A\beta_{1-42}$ peptide able to cross the BBB and target amyloid deposits in the brain of AD transgenic mice. Given the large size of the probe, several days (weeks) were necessary to label the amyloid plaques in the transgenic mouse brain in vivo.[19] Yang et al. detected amyloid deposition with iron oxide nanoparticles coupled to $A\beta_{1-42}$ peptide after intracarotid mannitol treatment to enhance BBB permeability in transgenic mice.[20]

Multimodality imaging combines two or more methodologies to provide complementary information. Optimally, the imaging probes used in the different modalities should possess identical biodistribution enabling an overlap of the acquired images. Metal ions provide suitable probes for various imaging modalities. By the appropriate choice of a chelating agent, one can complex, with the same ligand, different metal ions that possess properties for these imaging modalities. Provided their charge is identical, these complexes are expected to have similar biodistribution and are therefore interesting candidates for multimodal imaging applications.

Our objective was to design, synthesize, and investigate novel ligands with capability of (i) efficiently complexing metal ions adapted to different imaging modalities, including Gd^{3+} for MRI, $^{111}In^{3+}$ for SPECT, or $^{68}Ga^{3+}$ for PET; (ii) labeling $A\beta$ plaques via specific binding; and (iii) delivering the complexes across the BBB. We have conjugated a PiB derivative[21] to the metal chelating unit DO3A-monoamide. PiB derivatives are usually noncharged analogues of thioflavin T with excellent BBB permeability. $DOTA^{4-}$ derivatives are among the best chelators for many metal ions. They form highly stable and inert complexes, important for safe in vivo use. In our ligand design, the formation of neutral complexes with trivalent metal ions and a short linkage between the metal binding and the amyloid-recognition sites were essential elements to facilitate BBB permeability.

The synthesis of Ln(DO3A-PiB) complexes is summarized in Scheme 1 (see Supporting Information). Magnetic field dependent nuclear magnetic relaxation dispersion (NMRD) profiles are commonly used to characterize MRI contrast agents.[17] The NMRD curve of Gd(DO3A-PiB) recorded at 0.2 mM concentration is characteristic of a small-molecular weight complex (Figure 1).

Upon binding of Gd(DO3A-PiB) to $A\beta$ plaques, higher relaxivity is expected since the complex becomes immobilized. Indeed, in the presence of the amyloid peptide $A\beta_{1-40}$ ($c_{Gd} = c_{A\beta1-40} = 0.2$ mM), the relaxivity of Gd(DO3A-PiB) increases considerably at magnetic fields where the effect of slower rotation is most pronounced, evidencing an interaction. The

Scheme 1. Synthesis of Ln(DO3A-PiB)^a
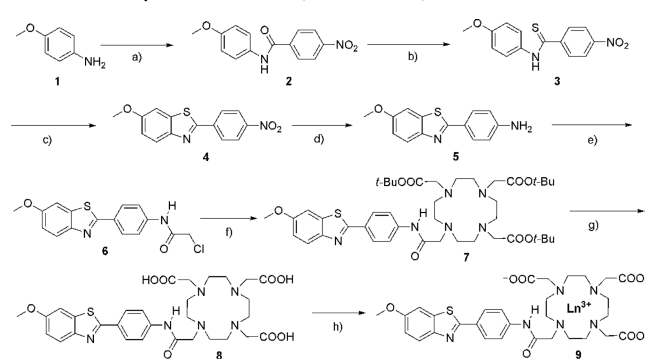
^{a}Reagents and conditions: (a) THF, NEt_3, 4-nitrobenzoyl chloride, 0°C, 96%; (b) chlorobenzene, Lawesson's reagent, reflux, 85%; (c) 10% NaOH, $K_3Fe(CN)_6$, reflux, 52%; (d) $SnCl_2$, EtOH, reflux, 92%; (e) $ClCH_2COCl$, K_2CO_3, CH_3CN, r.t., 86%; (f) tBu_3DO3A, K_2CO_3, CH_3CN, r.t., 88%; (g) dichloromethane, TFA, 45°C, 79%; (h) $GdCl_3$, pH 7.
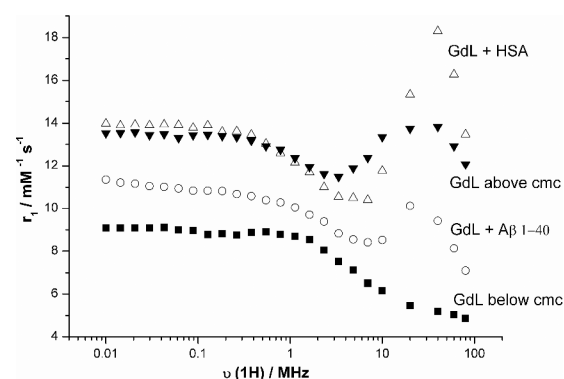

Figure 1. ^1H NMRD profiles of Gd(DO3A-PiB) at 0.2 mM (■), 5 mM (▼), 0.2 mM in the presence of 0.2 mM $A\beta_{1-40}$ (○), and 0.2 mM in the presence of 0.2 mM HSA (△) (0.05 M HEPES; pH 7.4, $T = 310$ K).

binding affinity of Gd(DO3A-PiB) to $A\beta_{1-40}$ was evaluated by surface plasmon resonance measurements (Figure S9, Supporting Information), which yielded $K_d = (180 \pm 10)$ μM, a value considerably higher than that for small benzothiazole derivatives ($K_d < 1$ μM).[22] Given their similar charge and the fact that the binding interaction mainly involves the PiB moiety, similar binding affinity is expected also for the Eu^{3+} and In^{3+} analogues. Gd(DO3A-PiB) binds to serum albumin as well, causing a remarkable increase of relaxivity at intermediate fields (Figures 1 and S1−S4, Supporting Information). Albumin binding leads to a prolonged lifetime of the agent in the blood pool that, given the slower elimination from the body, can be useful for an MRI probe, though unfavorable for nuclear imaging probes due to longer radiation exposure and higher nonspecific signal. Strong HSA binding can be also detrimental for the BBB permeability of the agent.[23] The binding affinity of Gd(DO3A-PiB) to HSA has been assessed by proton relaxation enhancement measurements and yielded $K_d = 110 \pm 20$ μM (Figures S1 and S2, Supporting Information).[24] The NMRD curve recorded at 5 mM Gd(DO3A-PiB) concentration shows the relaxivity peak at intermediate magnetic fields, typical of slowly tumbling systems thus evidencing the formation of micellar aggregates. A critical micellar concentration, $cmc = 1.90$

± 0.02 mM, was determined by relaxometry[25] (Figure S3, Supporting Information).

We tested the capability of Eu(DO3A-PiB) to bind amyloid aggregates on postmortem human brain tissue of AD patients. The staining with Eu(DO3A-PiB) revealed the presence of various amyloid deposits. The distribution pattern and intensity of the senile plaques were similar for PiB, thioflavin-S, and Eu(DO3A-PiB) (Figures S6 and S7, Supporting Information). Eu(DO3A-PiB) seems to have lower affinity for neurofibrillary tangles, being thus more specific to Aβ deposits than PiB (Figure 2). To confirm that PiB and Eu(DO3A-PiB) labeling is
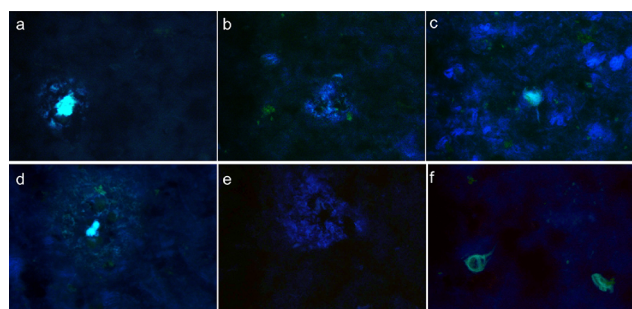

Figure 2. Positive staining of an Alzheimer tissue with PiB (a−c) and Eu(DO3A-PiB) (d−f). Senile plaques (left), diffuse deposits (middle), and neurofibrillary tangles (right) are put into evidence by the PIB and Eu(DO3A-PiB) staining.

specific for the amyloid deposits, we performed a double fluorescence staining experiment using the routinely employed 6F3D antibody (Figure 3). The staining of PiB and Eu(DO3A-
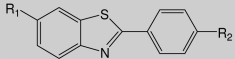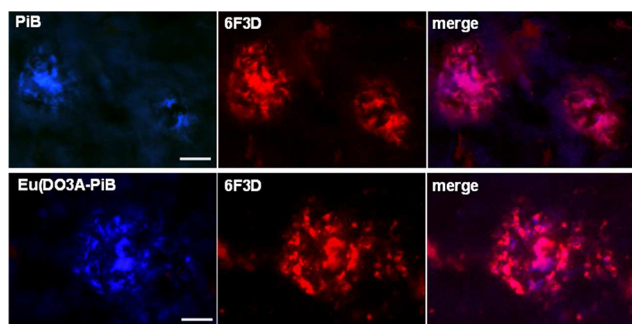

Figure 3. Micrographs illustrating the colocalization of PiB or Eu(DO3A-PiB) and 6F3D-antibody labeling of amyloid deposits of postmortem human brain tissue of an AD patient: the colocalization is confirmed by the magenta color in the merge images; scale bar = 20 μm.

PiB) is strong in the focal deposits, while the surrounding crown is slightly less positive, probably due to its partially fibrillar morphology. Some of the less intense Aβ positive structures were not labeled by PiB or Eu(DO3A-PiB).

The BBB permeability of a compound is related to its (i) lipophilicity, expressed by the water/octanol partition coefficient, log $P_{oct/water}$, (ii) molecular weight (MW), and (iii) plasma pharmacokinetics.[23] Low MW amphiphilic molecules with log $P_{oct/water} \approx 2$ have optimal BBB penetration. For Gd(DO3A-PiB), log $P_{oct/water} = -0.15$ was obtained, a value lower than that for phenylbenzothiazole derivatives (Table 1).[7,21,26] It is similar to those reported for neutral In(DTPA-bisamide) complexes bearing hydrophobic chains,[27] and higher than log $P_{oct/water} = -2.86$ for the double-charged In(DTPA)$^{2-}$.

Table 1. Molecular Weight (MW) and Lipophilicity (log $P_{Oct/H2O}$) of Phenylbenzothiazole (BTA) Derivatives

	log $P_{Oct/H2O}$	MW	Ref.
thioflavin T	0.57	319	7
R1 = CH$_3$, R2 = NH$_2$	2.6	240	7, 21
R1 = OCH$_3$, R2 = NH$_2$	1.9	256	7
R1 = CH$_3$, R2 = NHCH$_3$	2.6	254	7
R1 = OH, R2 = NHCH$_3$ (PiB)	1.23	256	26
R1 = OCH$_3$, R2 = ReOTEEDA	2.52	616	26
Gd(DO3A-PiB)	−0.15	842	this work

The molecular weight of Gd(DO3A-PiB), MW = 842, is above the optimal values,[28] although peptide analogues with a MW > 1000 Da were shown to cross the BBB.[29,30]

In order to evaluate the penetration of our complexes across the BBB, we have performed in vivo biodistribution experiments with the ^{111}In-analogue in adult male Swiss mice without amyloid deposits in their brain. The radiolabeling of the ligand has been carried out in isotonic ammonium acetate at pH 7.0, by adding a solution of ^{111}InCl$_3$ (specific activity 15.38 TBq/mg), to obtain 1:1 ^{111}In^{3+} complexes (10% ligand excess, 100 °C, 30 min). Thin layer chromatography indicated >96% radiochemical purity (Figure S7, Supporting Information). The complex remained stable in vitro with 2% degradation at 22 h after radiolabeling. The in vivo biodistribution of ^{111}In(DO3A-PiB) at 2 and 30 min (Table 2) showed the highest uptake in

Table 2. Distribution of ^{111}In(DO3A-PiB) in Swiss Mice 2 and 30 min after Tracer Injection; the Data Represent the Mean ± SD Percent Injected Dose Per Gram (% ID/g, $n = 4$)

% ID/g	2 min	30 min
kidney	12.53 ± 1.07	4.23 ± 0.42
cerebellum	0.50 ± 0.07	0.21 ± 0.02
cortex	0.36 ± 0.03	0.11 ± 0.01
heart	7.36 ± 0.18	1.51 ± 0.21
liver	4.90 ± 0.12	7.65 ± 1.59
blood	14.59 ± 0.23	4.23 ± 0.45
lung	11.42 ± 0.77	1.44 ± 0.14

kidney suggesting urinary elimination. The radioactive signal was also elevated in lungs 2 min after tracer injection, then decreased at the 30 min time point. This transient high lung uptake reflects the large blood volume of this blood-rich organ. In the brain, the % ID/g in the cortex and cerebellum at 2 min was 0.36 and 0.5, while at 30 min, it was 0.11 and 0.21, respectively. The clearance measured by the ratio of % ID/g values at 2 and 30 min is 3.3, comparable to that for PiB.[21] ^{99m}Tc-based β-amyloid tracers had similar or higher brain uptake (0.1−1.4% ID/g at 2 min and 0.1−1.08% ID/g at 30 min).[12−16] Given the higher molecular weight of ^{111}In(DO3A-PiB), the brain % ID/g values are remarkable. They are similar to the cerebral biodistribution of some SPECT radioligands, including PE2I[31] and CLINDE,[32] developed for brain imaging of the dopaminergic system and neuroinflammation. Therefore, the BBB crossing of ^{111}In(DO3A-PiB) might be sufficient for nuclear imaging amyloid deposits in rodent transgenic models overexpressing Aβ aggregates. BBB permeability sufficient for MRI detection with the Gd^{3+} analogue will be certainly difficult

438

dx.doi.org/10.1021/ml400042w | ACS Med. Chem. Lett. 2013, 4, 436−440

to attain. However, an MRI agent specifically binding to amyloid deposits can be useful in animal studies where a BBB opening is feasible. These agents can complete the use of nonspecific Gd-complexes like GdDTPA applied in intracerebroventricular injection protocols or can be useful in ex vivo MRI to stain Alzheimer brain tissues.[33]

In conclusion, we synthesized a novel amyloid targeted ligand, which is able to efficiently complex different metal ions adapted to various imaging modalities, including Gd^{3+} for MRI and $^{111}In^{3+}$ for SPECT. The complexes bind the amyloid peptide $A\beta_{1-40}$. This results in elevated relaxivity of the Gd^{3+} analogue due to reduced rotational motion, which will lead to an increased contrast in T_1-weighted images upon binding to senile plaques. The complexes show affinity for amyloid deposits in postmortem human tissue. The biodistribution experiments in normal mice proved moderate brain uptake.

■ ASSOCIATED CONTENT

Ⓢ Supporting Information

Synthesis, immunohistochemistry, relaxometric studies, and experimental procedures. This material is available free of charge via the Internet at http://pubs.acs.org.

■ AUTHOR INFORMATION

Corresponding Authors

*(C.F.G.C.G.) Department of Life Sciences, University of Coimbra, P.O. Box 3046, 3001-401 Coimbra, Portugal. E-mail: geraldes@ci.uc.pt. Fax: (+351) 2 39 85 36 07.
*(É.T.) E-mail: eva.jakabtoth@cnrs-orleans.fr. Fax: (+33) 2 38 63 15 17.

Author Contributions

The manuscript was written through contributions of all authors. All authors have given approval to the final version of this manuscript.

Notes

The authors declare no competing financial interest.

■ ABBREVIATIONS

AD, Alzheimer's disease; CA, contrast agent; MRI, magnetic resonance imaging; PET, positron emission tomography; SPECT, single-photon emission computed tomography; BBB, blood brain barrier; HSA, human serum albumin; MW, molecular weight; PiB, Pittsburgh compound B

■ REFERENCES

(1) Evans, D. A.; Funkenstein, H. H.; Albert, M. S. Prevalence of Alzheimers-disease in a community population of older persons: higher than previously reported. *JAMA* **1989**, *262*, 2551−2556.
(2) Fratiglioni, L.; Winblad, B.; von Strauss, E. Prevention of Alzheimer's disease and dementia. Major findings from the Kungsholmen project. *Physiol. Behav.* **2007**, *92*, 98−104.
(3) American Psychiatric Association. *Diagnostic and Statistical Manual of Mental Disorders*, 4th ed; American Psychiatric Association: Washington, DC, 2000.
(4) Braak, H.; Braak, E. Neuropathological staging of Alzheimer-related changes. *Acta Neuropathol.* **1991**, *82*, 239−259.

(5) Hardy, J.; Selkoe, D. J. Medicine: The amyloid hypothesis of Alzheimer's disease: Progress and problems on the road to therapeutics. *Science* **2002**, *297*, 353−356.
(6) Rauk, A. The chemistry of Alzheimer's disease. *Chem. Soc. Rev.* **2009**, *38*, 2698−2715.
(7) Mathis, C. A.; Bacskai, B. J.; Kajdasz, S. T.; McLellan, M. E.; Frosch, M. P.; Hyman, B. T.; Holt, D. P.; Wang, Y.; Huang, G. F.; Debnath, M. L.; Klunk, W. E. A lipophilic thioflavin-T derivative for positron emission tomography (PET) imaging of amyloid in brain. *Bioorg. Med. Chem. Lett.* **2002**, *12*, 295−298.
(8) Vandenberghe, R.; Van Laere, K.; Ivanoiu, A.; Salmon, E.; Bastin, C.; Triau, E.; Hasselbalch, S.; Law, I.; Andersen, A.; Korner, A.; Minthon, L.; Garraux, G.; Nelissen, N.; Bormans, G.; Buckley, C.; Owenius, R.; Thurfjell, L.; Farrar, G.; Brooks, D. J. 18F-Flutemetamol amyloid imaging in Alzheimer disease and mild cognitive impairment: a phase 2 trial. *Ann. Neurol.* **2010**, *68*, 319−29.
(9) Camus, V.; Payoux, P.; Barré, L.; Desgranges, B.; Voisin, T.; Tauber, C.; La Joie, R.; Tafani, M.; Hommet, C.; Chételat, G.; Mondon, K.; de La Sayette, V.; Cottier, J. P.; Beaufils, E.; Ribeiro, M. J.; Gissot, V.; Vierron, E.; Vercouillie, J.; Vellas, B.; Eustache, F.; Guilloteau, D. Using PET with 18F-AV-45 (florbetapir) to quantify brain amyloid load in a clinical environment. *Eur. J. Nucl. Med. Mol. Imaging* **2012**, *39*, 621−631.
(10) Barthel, H.; Gertz, H. J.; Dresel, S.; Peters, O.; Bartenstein, P.; Buerger, K.; Hiemeyer, F.; Wittemer-Rump, S. M.; Seibyl, J.; Reininger, C.; Sabri, O.; et al. Cerebral amyloid-β PET with florbetaben (^{18}F) in patients with Alzheimer's disease and healthy controls: a multicentre phase 2 diagnostic study. *Lancet Neurol.* **2011**, *10*, 424−435.
(11) Nesterov, E. E.; Skoch, J.; Hyman, B. T.; Klunk, W. E.; Bacskai, B. J.; Swager, T. M. In vivo optical Imaging of amyloid aggregates in brain: Design of fluorescent markers. *Angew. Chem., Int. Ed.* **2005**, *26*, 5452−5456.
(12) Zhuang, Z. P.; Kung, M. P.; Hou, C.; Ploessl, K.; Kung, H. F. Biphenyls labeled with technetium 99m for imaging β-amyloid plaques in the brain. *Nucl. Med. Biol.* **2005**, *32*, 171−184.
(13) Serdons, K.; Verduyckt, T.; Cleynhens, J.; Terwinghe, C.; Mortelmans, L.; Bormans, G.; Verbruggen, A. Synthesis and evaluation of a [^{99m}Tc]-BAT-phenylbenzothiazole conjugate as a potential in vivo tracer for visualization of amyloid β. *Bioorg. Med. Chem. Lett.* **2007**, *17*, 6086−6090.
(14) Ono, M.; Ikeoka, R.; Watanabe, H.; Kimura, H.; Fuchigami, T.; Haratake, M.; Saji, H.; Nakayama, M. Synthesis and evaluation of novel chalcone derivatives with 99mTc/Re complexes as potential probes for detection of β-amyloid plaques. *ACS Chem. Neurosci.* **2010**, *1*, 598.
(15) Ono, M.; Ikeoka, R.; Watanabe, H.; Kimura, H.; Fuchigami, T.; Haratake, M.; Saji, H.; Nakayama, M. ^{99m}Tc/Re complexes based on flavone and aurone as SPECT probes for imaging cerebral β-amyloid plaques. *Bioorg. Med. Chem. Lett.* **2010**, *20*, 5743−5748.
(16) Cheng, Y.; Ono, M.; Kimura, H.; Ueda, M.; Saji, H. Technetium-99m labeled pyridyl benzofuran derivatives as single photon emission computed tomography imaging probes for β-amyloid plaques in Alzheimer's brains. *J. Med. Chem.* **2012**, *55*, 2279−2286.
(17) Toth, E.; Merbach, A., Eds. *The Chemistry of Contrast Agents in Medical MRI*; John Wiley & Sons: Chichester, U.K., 2001.
(18) Jack, C. R.; Garwood, M.; Wengenack, T. M.; Borowski, B.; Curran, G. L.; Lin, J.; Adriany, G.; Grohn, I. H. J.; Grimm, R.; Poduslo, J. F. In vivo visualization of Alzheimer's amyloid plaques by magnetic resonance imaging in transgenic mice without a contrast agent. *Magn. Reson. Med.* **2004**, *52*, 1263−1271.
(19) Poduslo, J. F.; Wengenack, T. M.; Curran, G. L.; Wisniewski, T.; Sigurdsson, E. M.; Macura, S. I.; Borowski, B. J.; Jack, C. R., Jr. Molecular targeting of Alzheimer's amyloid plaques for contrast-enhanced magnetic resonance imaging. *Neurobiol. Dis.* **2002**, *11*, 315−329.
(20) Yang, J.; Wadghiri, Y. Z.; Hoang, D. M.; Tsui, W.; Sun, Y. J.; Chung, E.; Li, Y. S.; Wang, A.; de Leon, M.; Wisniewski, T. Detection of amyloid plaques targeted by USPIO-A beta 1-42 in Alzheimer's

439

dx.doi.org/10.1021/ml400042w | *ACS Med. Chem. Lett.* 2013, 4, 436−440

disease transgenic mice using magnetic resonance microimaging. *Neuroimage* **2011**, *55*, 1600−1609.

(21) Mathis, C. A.; Wang, Y.; Holt, D. P.; Huang, G.-F.; Debnath, M. L.; Klunk, W. E. Synthesis and evaluation of C-11-labeled 6-substituted 2-arylbenzothiazoles as amyloid imaging agents. *J. Med. Chem.* **2003**, *46*, 2740−2754.

(22) Yona, R. L.; Mazères, S.; Faller, P.; Gras, E. Thioflavin derivatives of amyloid-*β* fibrils: insights into structural features important for high-affinity binding. *ChemMedChem* **2008**, *3*, 63−66.

(23) Mensch, J.; Oyarzabal, J.; Mackie, C.; Augustijns, P. In vivo, in vitro and in silico methods for small molecule transfer across the BBB. *J. Pharm. Sci.* **2009**, *98*, 4429−4468.

(24) Aime, S.; Fasano, M.; Terreno, E., Botta, M. Protein-Bound Metal Chelates. In *The Chemistry of Contrast Agents in Medical Magnetic Resonance Imaging*; Merbach, A.E., Toth, E., Eds.; Wiley: New York, 2001; Chapter 5, pp 194−241.

(25) Nicolle, G. M.; Tóth, É.; Eisenwiener, K.-P.; Mäcke, H. R.; Merbach, A. E. From monomers to micelles: investigation of the parameters influencing proton relaxivity. *J. Biol. Inorg. Chem.* **2002**, *7*, 757−769.

(26) Lin, K.-S.; Debnath, M. L.; Mathis, C. A.; Klunk, W. E. Synthesis and beta-amyloid binding properties of rhenium 2-phenylbenzothiazoles. *Bioorg. Med. Chem. Lett.* **2009**, *19*, 2258−2262.

(27) Prata, M. I. M.; Santos, A. C.; Bligh, S. W. A.; Chowdhury, A. H. M. S.; Geraldes, C. F. G. C.; de Lima, J. J. P. Characterization of In-111(3+) complexes of DTPA amide derivatives: Biodistribution and clearance studied by gamma imaging. *Nucl. Med. Biol.* **2000**, *27*, 605−610.

(28) Levin, V. Relationship of octanol−water partition-coefficient and molecular-weight to rat brain capillary-permeability. *J. Med. Chem.* **1980**, *23*, 682−684.

(29) Bornebroek, M.; Verzijlbergen, J.; Haan, J.; Van Scheyen, E.; Verhoeff, N.; Pauwels, E.; Roos, R. Potential for imaging cerebral amyloid deposits using I-123-labelled serum amyloid P component and SPET. *Nucl. Med. Commun.* **1996**, *17*, 929−933.

(30) Saito, Y.; Buciak, J.; Yang, J.; Pardridge, W. M. Vector-mediated delivery of I-125 labeled beta-amyloid peptide A-beta(1−40) through the blood-brain-barrier and binding to Alzheimer-disease amyloid of the A-beta(1−40)/vector complex. *Proc. Natl. Acad. Sci. U.S.A.* **1995**, *92*, 10227.

(31) Emond, P.; Guilloteau, D.; Chalon, S. PE2I: a radio-pharmaceutical for in vivo exploration of the dopamine transporter. *CNS Neurosci. Ther.* **2008**, *14*, 47−64.

(32) Arlicot, N.; Katsifis, A.; Garreau, L.; Mattner, F.; Vergote, J.; Duval, S.; Kousignian, I.; Bodard, S.; Guilloteau, D.; Chalon, S. Evaluation of CLINDE as potent translocator protein (18 kDa) SPECT radiotracer reflecting the degree of neuroinflammation in a rat model of microglial activation. *Eur. J. Nucl. Med. Mol. Imaging* **2008**, *35*, 2203−2211.

(33) Petiet, A.; Dhenain, M. Improvement of microscopic MR imaging if amyloid plaques with targeting and non-targeting contrast agents. *Curr. Med. Imaging Rev.* **2011**, *7*, 1−8.